410

Archi-Cultural Translations through the Silk Road
2nd International Conference, Mukogawa Women's Univ., Nishinomiya, Japan, July 14-16, 2012
Proceedings

SEISMIC PERFORMANCE AND REINFORCEMENT OF JAPANESE HIGH-RISE BUILDINGS FACING SUBDUCTION EARTHQUAKE: E-DEFENSE SHAKE TABLE TESTS

Takuya Nagae[1], Masayoshi Nakashima[2]

[1] *National Research Institute for Earth Science and Disaster Prevention, Japan*
[2] *Kyoto University, Japan*

Keywords: Subduction earthquake, high-rise building, large-scale test.

Introduction

Periodical occurrences of large ocean-ridge earthquakes having a magnitude over eight along the subduction zones in the southwest part of Japan have been documented in historical materials. Such earthquakes are known to generate long-period ground motions on land, especially in the basin areas where large cities such as Tokyo, Nagaya and Osaka are located. Their predominant periods range from several to ten seconds, and the durations of primary motion extend over several minutes. Long-period ground motions tend to resonate high-rise buildings whose fundamental natural periods are several seconds. Because high-rise buildings, which concentrate in large cities, perform very important roles in the Japanese economy, severe damage to them shall cause extreme difficulties throughout Japan. The seismic performance of existing high-rise buildings should be evaluated with urgency. However because the high-rise buildings have never experienced long-period ground motions before, no actual data have been available on possible seismic damage. This is the primary motivation of this study.

Capacity of the E-Defense shaking table and design of the test specimen

The E-Defense shaking table is 20 m by 15 m in plan dimension and can produce a velocity of 2.0 m/s and a displacement of 1.0 m in two horizontal directions simultaneously. It can accommodate a specimen up to a weight of 1,200 metric tons and a height of 22 m.
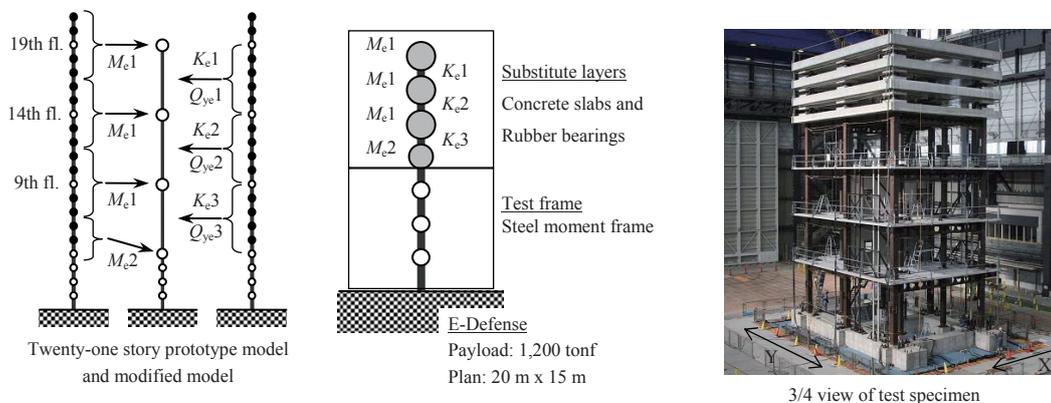
Fig. 1: Development of test method

Fig. 1 shows the test method employed in this study. The concept adopted for this test was to establish a partial frame structure having full-scale steel members and being able to reproduce the possible seismic responses of a prototype building that has twenty-one stories with a total height of 80 m. The test specimen consists of a four-story, two-span by one-bay steel moment frame and three substitute layers placed on top of the moment frame. The substitute layers, which consist of concrete slabs and rubber bearings, are arranged to represent the upper stories of the prototype. From preliminary vibration tests, equivalence between the test specimen and the prototype was verified in terms of the lower mode natural periods and corresponding mode shapes. The natural period of the test specimen was 2.1 sec. By using this test method, a series of large-scale shaking table tests were planned for a high-rise building subjected to long-period ground motions.

Seismic performance of existing high-rise steel buildings (The 2008 E-Defense test)

Fig. 2 shows the beam-to-column connection details. Typical design and detailing in the 1970's are incorporated in a four-story, steel moment frame specimen. For the tests, two synthesized long period ground motions were adopted. The HOG-wave (PGA=1.45 m/s^2, PGV= 0.40 m/s) was predicted at a Kawasaki site, where is next to Tokyo, and rupture of the Tokai trough was supposed. The SAN-wave (PGA=1.86 m/s2, PGV= 0.51 m/s) was predicted at a Nagoya site, and simultaneous ruptures of the Tokai and Tounankai troughs were supposed. In addtion, EL2-wave scaled to PGV of 0.5 m/s was adopted, as that has been used as the level 2 seismic force in the Japanese seismic design.

(a) Shop-weld connection
(Y-direction)

(b) Field-weld connection   (X-direction)
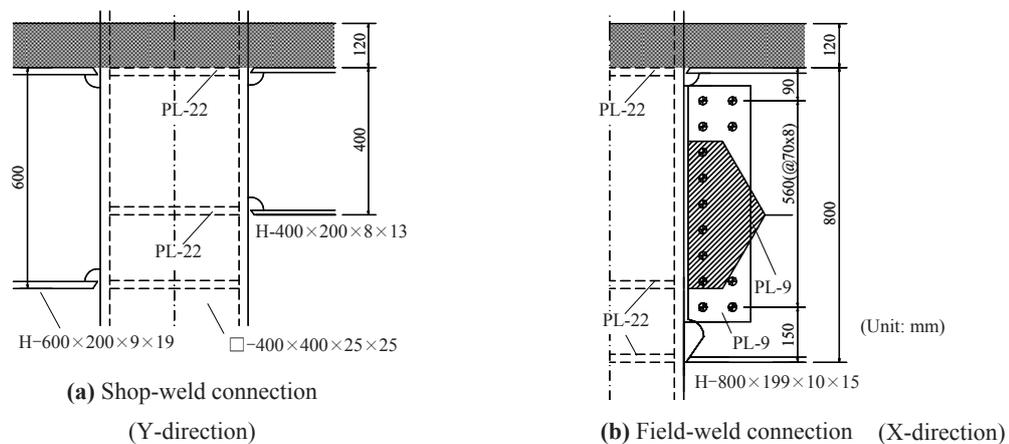
Fig. 2: Beam-to-column connections

First, the EL-2 wave was applied, and then the HOG wave and the SAN-wave were applied sequentially. Fig. 3 shows the seismic response of the test specimen. For the EL2-wave, the maximum inter-story drift was slightly smaller than the design limit of 0.01 rad. For the HOG-wave and SAN-wave, the maximum inter-story drifts was 0.011 rad and 0.017 rad. On the other hand, the test specimen when subjected to the HOG-wave and SAN-wave exhibits larg input energy more than four times that of the EL2-wave in the durations of 200 and 320 sec. Fig. 4 shows bending moment versus rotation relations (M-θ relations) at beam ends. In the first test of SAN-wave, fractures of beam ends occurred at three field-weld connections (WUF-B) arranged in the X-direction, while no obvious damage was observed in the shop

weld connections placed in the Y-direction. Eventually, two more tests were conducted for the fracture of the shop weld connection in Y-direction. As the maximum strain value at the bottom flange was confirmed as significantly larger the upper flange, the bottom flange fracture was attributed to the amplified strains due to the composite effect of the RC floor slabs as well as the large cumulative inelastic deformations.

(a) Inter-story drift angle (Y-direction) **(b)** Input energy (Y-direction)
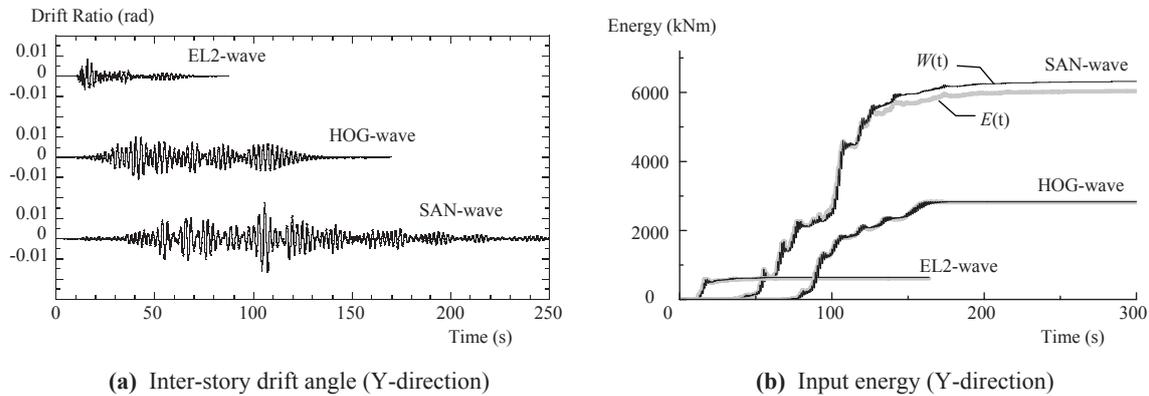
Fig. 3: Seismic response of test specimen

(a) Shop-weld connection (SAN-wave was input three times in Y-direction) **(b)** Field-weld connection
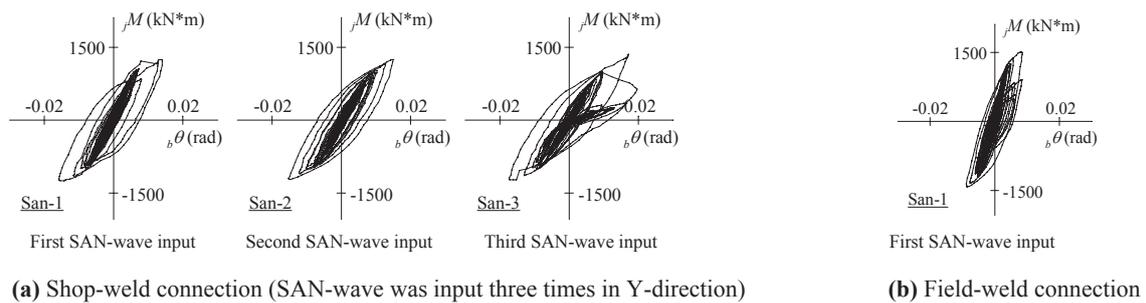
Fig. 4: Bending moment versus rotation relationships (M-θ relationships) at the beam ends

Reinforcement of high-rise steel buildings (The 2009 E-Defense test)

Fig. 5 shows the concept of the 2009 E-Defense test, in which the test specimen was reinforced with seismic dampers system. In the Case-I and Case-II for steel damper series, Buckling-Restrained Brace dampers were incorporated in the lower steel frame, and modeled steel dampers were utilized for the substitute layers. In the Case-III for oil damper series, oil dampers in diagonal braces were incorporated in the lower steel frame. In the SAN-wave, the maximum story drift angles of specimen were reduced to less than 1 % by dampers. Fig. 6 shows the force-deformation hysteresis and energy absorption of dampers. In the test frame, the energy was absorbed more than 70 % by the steel dampers or the oil dampers. As for the BRB damper, the cumulative inelastic strain capacity was estimated about ten times larger than the seismic demand in SAN-wave.
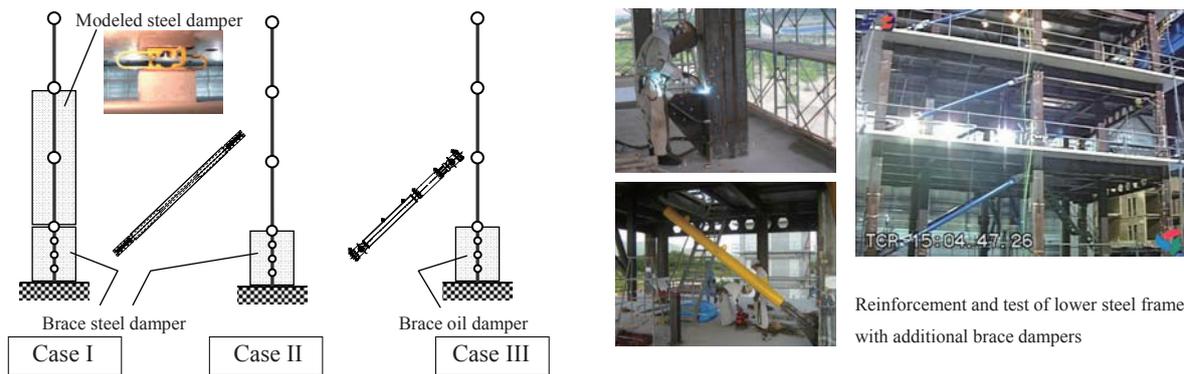
Fig. 5: Concept of the 2009 test on high-rise building reinforced by dampers

In the end, seismic performance of reinforced beam-to-column connections were examined in the test frame with no damper. Fig. 7 shows three types of reinforcement for field-weld beam-to-column connection. The deformation capacity was highly enhanced by those applicable reinforcement methods as shown in Fig. 8.

Fig. 9 shows the energy spectrum of input waves. The spectrum was given by the elastic SDOF with the damping ratio of 10 %. In this test series, the HOG-wave and the SAN-wave were adopted as the typical long period ground motion. These two waves had predominant magnitudes at around three seconds, while EL2-wave had a flat shape. The total input energies of the test specimen with no dampers as well as the test specimens characterized by Case-I, Case-II and Case-III reasonably correspond to the estimations of energy spectra at each natural period.

According to the test results, the reinforcement policies of existing high-rise buildings are derived;

(1)   Estimate input energy demand from energy spectra of long period ground motions
(2)   Reduce energy absorption of steel frame by reinforcement with dampers
(3)   Increase of cumulative inelastic deformation capacity of steel frame by reinforcing beam-to column connections (especially field-weld connections)

(a) Steel damper
(Case II, SAN-wave)

(b) Oil damper
(Case III, SAN-wave)

(c) Steel damper
(Case II)

(d) Oil damper
(Case III)
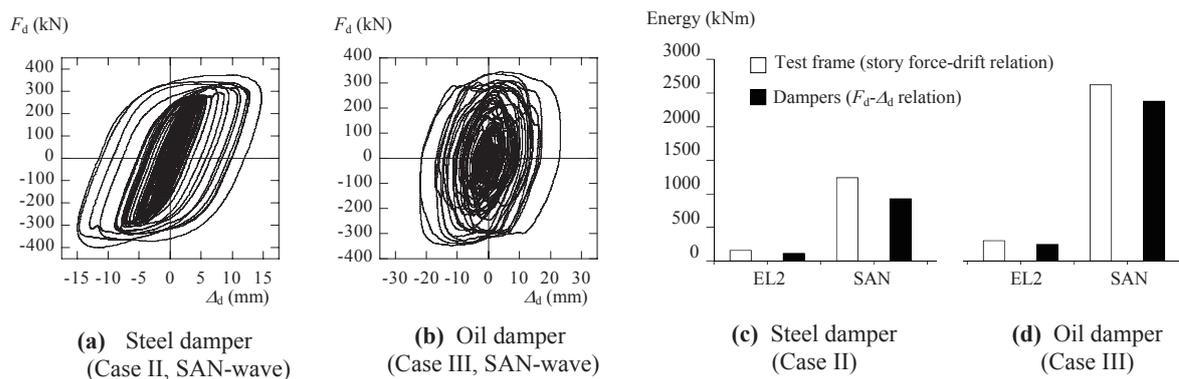
Fig. 6: Force-deformation relationship of dampers ((a), (b)), energy absorption of test frame and dampers ((c), (d))

(a) M-W connection

(b) WP-W connection

(c) H-W connection

(d) Procedure of WP-W connection
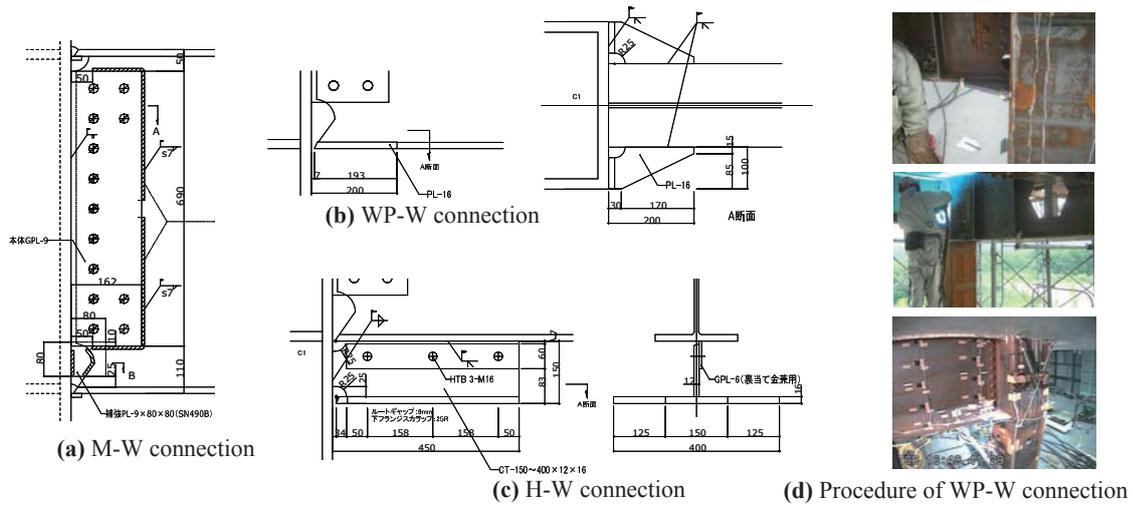
Fig. 7: Reinforcement of field-welded beam-to-column connection

$$\Sigma_b \theta_p = \sum_{i=1}^{N} {}_b\theta_{pi}$$
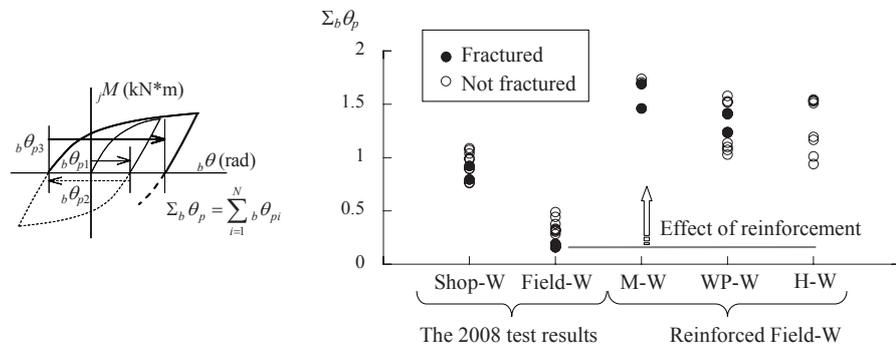
Fig. 8: Cumulative deformation capacity of beam-to-column

● Steel damper (Case-I) ▲ Steel damper (Case-II) ◆ Oil damper (Case-III) ○ No damper (2008)
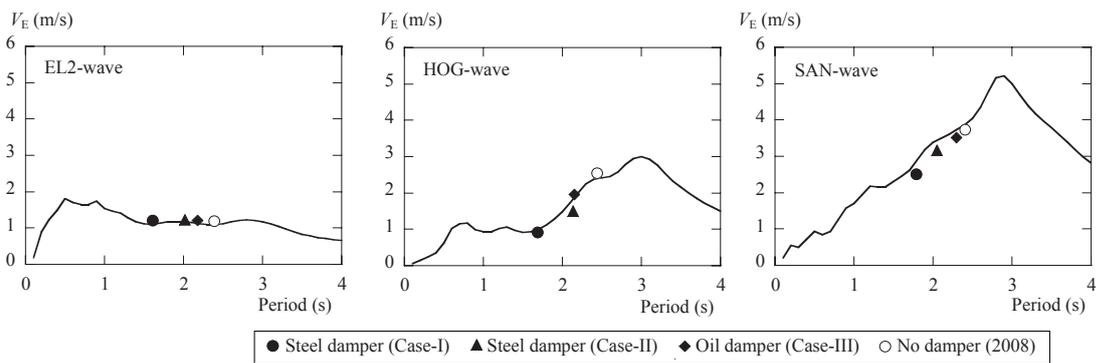
Fig. 9: Energy spectra and test results

244